Project Report

Abhijit Chakraborty

July 16, 2015

Abstract

Binary stars play significant role in the dynamical evolution of stellar clusters. The effect of interaction of a star from the cluster with the binary has been studied before in detail, but using the Newtonian formalism. We have used the Post-Newtonian model here to study the effect of the interaction of the star with the binary and compare them with the classical results. Also a different algorithm developed by Seppo Mikkola has been used instead of the usual leap frog integrator method to carry out the integrations.

1 Introduction

Interaction of binary stars and a 3rd-body (star from the surrounding cluster) can be considered as the energy exchange between two systems. As long as the binary is bound, the orbit of the reduced particle is a Kepler ellipse with semi major axis 'a' and the internal energy is given by $E = -\frac{Gm_1m_2}{2a}$ where m_1 and m_2 are the masses of the two binary stars. Now during an interaction of a binary with a star, the star can either extract energy from the binary, and thus increasing its kinetic energy or it can lose a fraction of its energy to the binary which is converted into the binding energy of the binary. Now, out of the two scenarios which is more likely to happen depends on the internal energy of the binary. Hard binaries which have binding energies exceeding the mean kinetic energy per star in the stellar cluster tend to act as energy providers to the star and in the process becomes harder and for soft binaries having binding energies smaller than the average kinetic energy of the cluster tend to gain energy from the star and expand. This phenomenon is known as Heggie's Law[1].
However all the simulations that led to the results are done using Newtonian energy formalism and thus neglecting the post-Newtonian effect and the energy loss due to Gravitational radiation. In this project, we want to investigate how the binding energy of the binary changes when it interacts with a star and build up a statistics of the energy change if we consider the post-Newtonian terms of order 1, 2 and 2.5 (as an approximation for the Einstein field equations for the binary). Also we want to compare the results with the No-PN case to see the difference.

2 Simulations

The integration algorithm that has been used in our study is developed by Seppo Mikkola[2] which is based on the chain regularization algorithm and is faster and more

accurate than the traditional leap-frog integration method. The validity of the method has been verified by checking the energy conservation. In the simulations we have used standard units for mass and distance which is 10^9 solar mass and 100 parsec and G is taken to be 1. With these units, the velocity of light is c = 477.12 units. The binary components are black holes with masses 3.2670693472027779E-03 mass units and 8.7121763499453664E-04 mass units respectively. The field star mass is taken as 10^{-7} mass units. The initial position and velocity of the binaries are obtained from available black-hole binary data and the initial position of the star is taken to distributed on a sphere of radius 0.1 unit with centre of the sphere at the C.o.M. of the binary. For the first set of runs the initial velocity has been fixed and is given by $0.01 \times V_{esc}$ where V_{esc} is the escape velocity given by $V_{esc} = \sqrt{\frac{2GM_{12}}{D}}$ where D = 0.1 length units and M_{12} is the total mass of the binary. For the next set of runs, the initial velocity is dependent on the pericenter distance which is a parameter of our simulations. The initial velocity is determined by the following formula

$$V = \sqrt{\frac{(1-e)M_{12}}{(1+e)a}} \tag{1}$$

where a and e are given by:
$a = \frac{D+ka_0}{2}$ and $e = \frac{D-ka_0}{D+ka_0}$. Here D is the apocenter distance (D=0.1 length units), a_0 is the initial binary semi major axis and k is a multiplier. The simulations are repeated for different initial conditions of the binary, i.e. for different snapshots of the binary for t=2,3,4,5 and 6. The integration is carried out until the star is ejected from the system (i.e. total energy of the star is positive) or upto a time period of t=100 with time steps dt = 0.01.
The formulae used to calculate the PN energies are same as mentioned in L. Blanchet and B.R. Iyer (2003) paper[3]. The gravitational radiation loss is cross-checked with P.C. Peters formula of change in semi-major axis of binary orbit[4].

3 Observation and Analysis

3.1 Energy Conservation

To show the energy conservation and validity of the code we have plotted the difference in total energy of the system for each time step. As we can see from figure 1, the order of error in energy conservation is at max of the order 10^{-5}. So, the accuracy is to the order of 0.1%. The total energy of the system that must be conserved is taken as B.E. of the binary + total energy of the star where B.E. consists of the PN1,2,2.5 terms along with the newtonian terms.

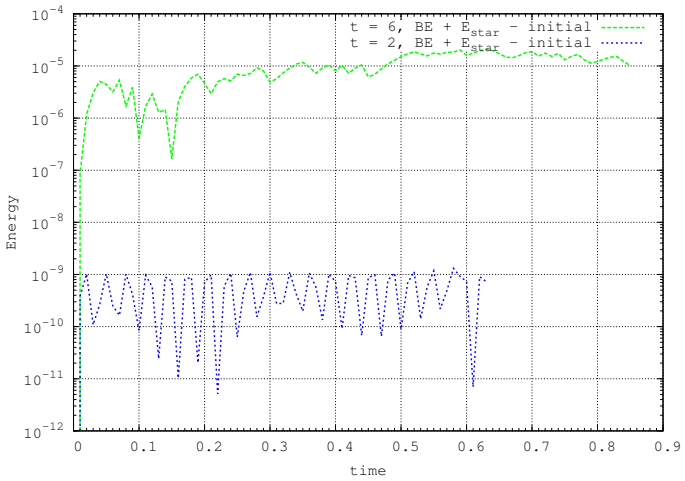

Figure 1: Energy conservation

3.2 Trajectory of the star

Next we show the trajectory of the star for a single run. The trajectory shows the interaction of the star with the binary and finally it gets ejected from the system. Fig. 2,3, and 4 shows the variation of three co-ordinates with time and Fig.5 shows the X-Y plot.

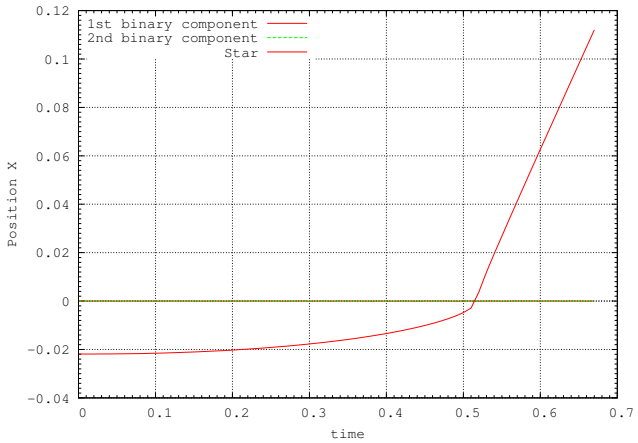

Figure 2: X vs t plot

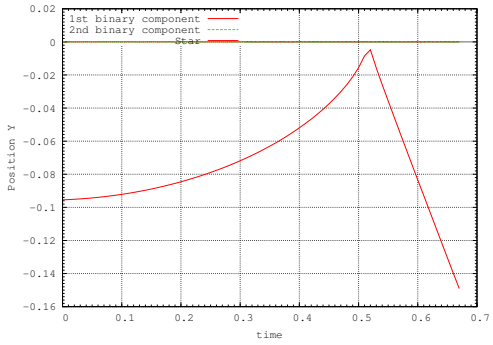

Figure 3: Y vs. t plot

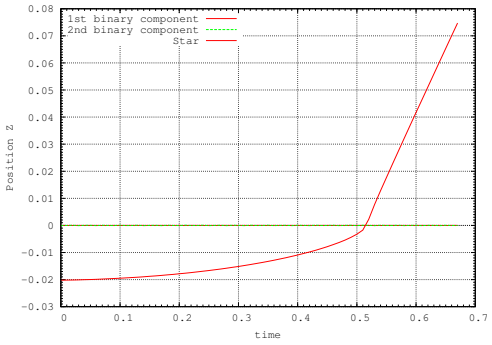

Figure 4: Z vs. t plot

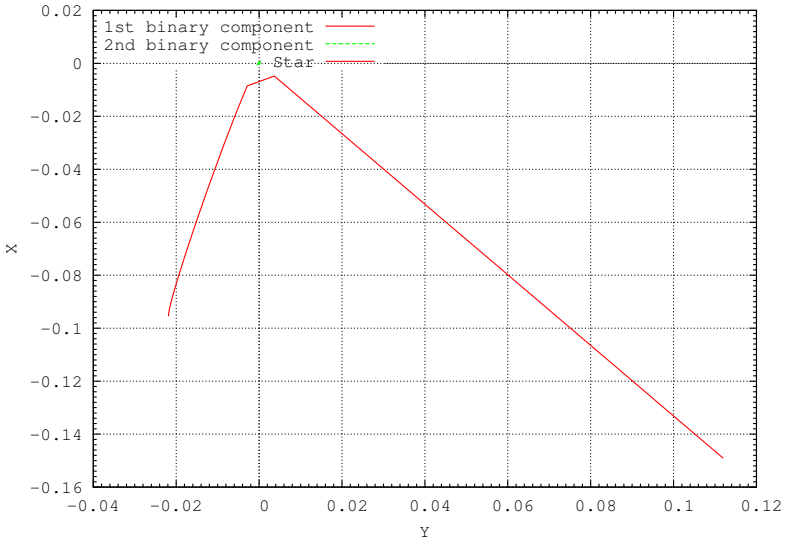

Figure 5: X vs Y plot

3.3 Energy Change in a single interaction

To show the variation of energy change in a single interaction, we have plotted the binding energy variation of the binary with time (Fig.6).

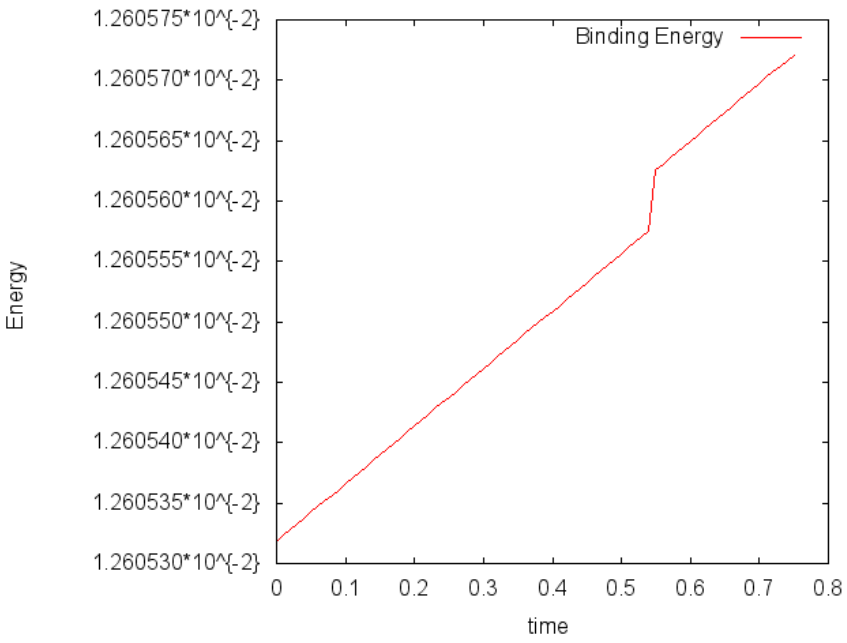

Figure 6: Binding energy (Newt+PN1+PN2) of the binary

The sudden jump indicates the ejection of the star from the system. This shows that the binary becomes harder after the ejection of the star.
To show that the kinetic energy of the star increases after the interaction we have plotted the variation of kinetic energy of the star with time.

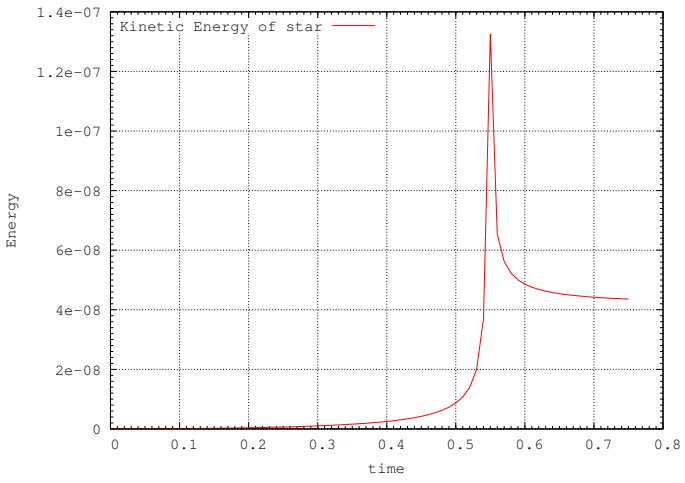

Figure 7: Kinetic energy of the star

Though the kinetic energy of the center of mass is almost negligible, it also receives an increase in energy as shown in Fig.8.

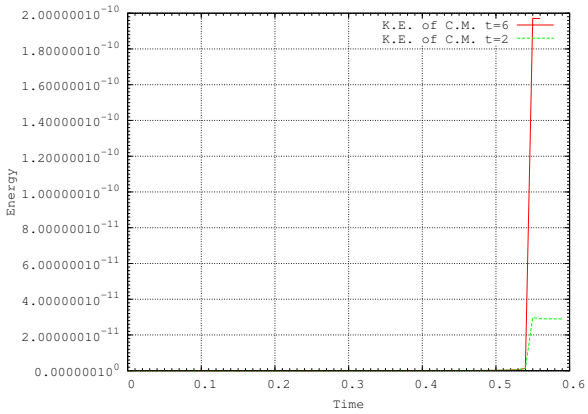

Figure 8: Change in center of mass kinetic energy of BBH

3.4 PN 2.5 term

The PN 2.5 term corresponds to the quadrupole moment of the gravitational field (given by Einstein). This 2.5 term (due to the $1/c^5$ dependence) indicates how much energy is lost due to the gravitational radiation from the binaries. This approximation is valid only for weak fields, but applies quite appropriately for the binary black hole case. The 2.5PN term has been calculated using Blanchet's formula (See ref. [3]). But this is cross-checked with the formula of Peters (See ref. [4]) which gives the variation of 'a', the semi-major axis of the binary, with time.

Fig 9. shows the comparison of the energy change due to gravitational radiation as

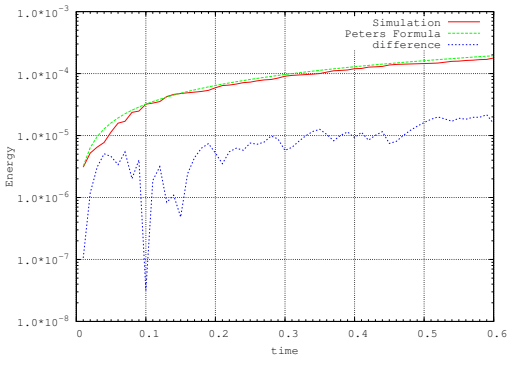

Figure 9: Comparison of Peters' formula of energy change and 2.5PN (y in logscale)

calculated by the two different formula. The evaluation of change in 'a' is calculated using Euler integration method (to integrate $\frac{da}{dt}$) and then it is multiplied by $\frac{Gm_1m_2}{2}$ (i.e.$\Delta E = -\frac{Gm_1m_2}{2}\int_0^t \frac{da}{dt}$). It can be that due to the first order approximation in integration we see the slight difference between the two approach.
Now, to show how the PN2.5 term depends on time-scale, we present Fig. 10.
As can be seen, the effect of PN2.5 term is more prominent in the case of t=6 than

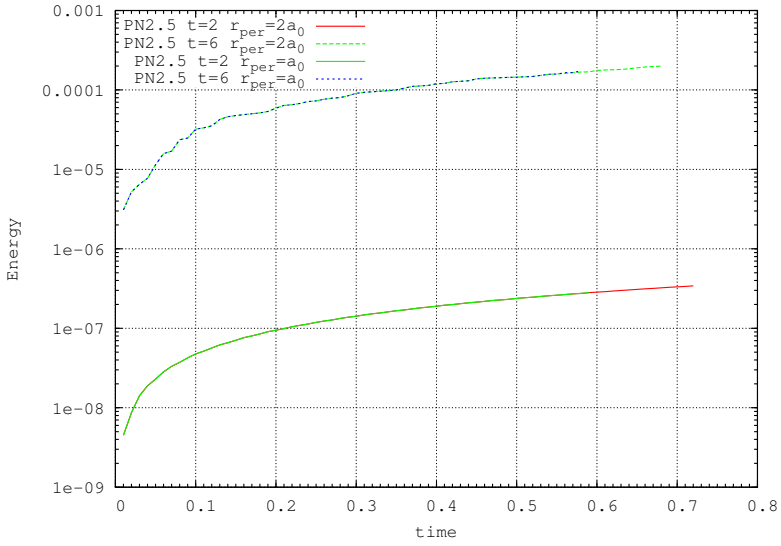

Figure 10: Effect of PN 2.5 terms for different cases

t=2 case which is understandable, but it does not depend on the 3rd-body's velocity of approach.

3.5 Effect of the PN 2.5 term

Fig. 11 and Fig.12 shows the effect of the PN2.5 term on the total energy and how the binding energy changes if we add the PN 2.5 term to Newtonian + PN1 +PN2 energy. As we can see that the effect of PN2.5 is really small. The PN2.5 energy is only about 0.5% of the total energy.

In all the sections that follows we have used the corrected energy i.e. Newtonian + PN1 + PN2 energy to calculate the cumulative energy and plot the differential distrbution. If only the word 'energy' is mentioned, it means this corrected energy.

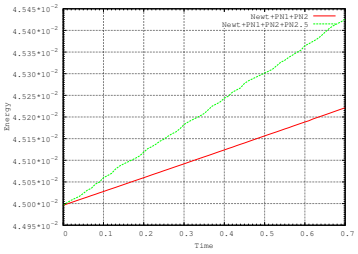

Figure 11: Time variation of Newt+PN1+PN2 and Newt+PN1+PN2+PN2.5 for a single run

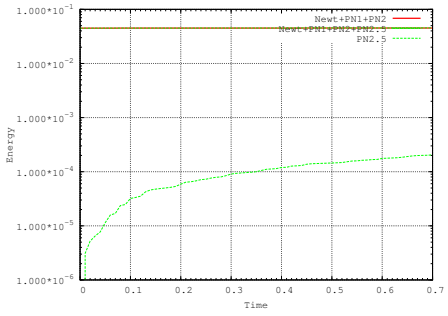

Figure 12: Comparison of PN2.5 energy with Newt+PN1+PN2 (y in logscale)

3.6 Comparison of cumulative energy change

This part provides the idea of the how much the energy change in an interaction on an average. Three parameters are considered here for the comparison. The parameters are, a) different initial position for the binaries (t=2 and t=6 case), b) different velocity of approach for the intruder (corresponding to different pericenter distance a_0 and $2a_0$) and c) PN, No-PN case. a_0 for t = 6 is 3.153813835E-005 and for t = 2 is 1.12812866E-004. Ellipticity of the binary orbit: for t=2, e_0 = 2.6203501433E-002, and for t=6, e_0 = 0.147133170924

The binding energy in case of PN activated simulations are calculated using Blanchet's formula of energy[5], and in case of No-PN, simple Newtonian formalism has been used to calculate the binary binding energy (given by $\frac{Gm_1m_2}{2a}$).

PN-NoPN comparison

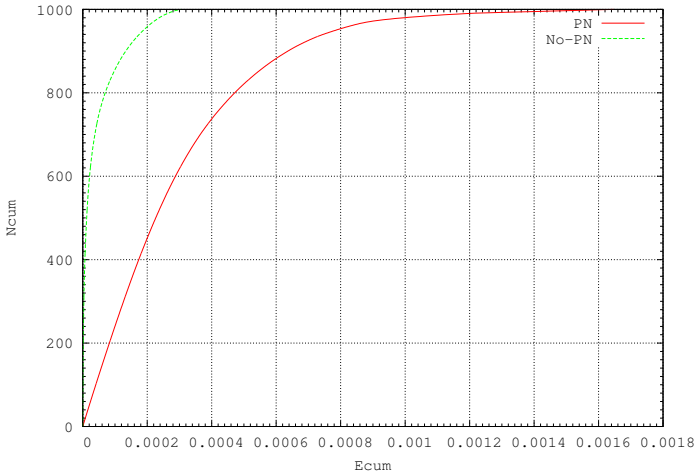

Figure 13: for t=2, $r_{per} = 2a_0$, cumulative energy

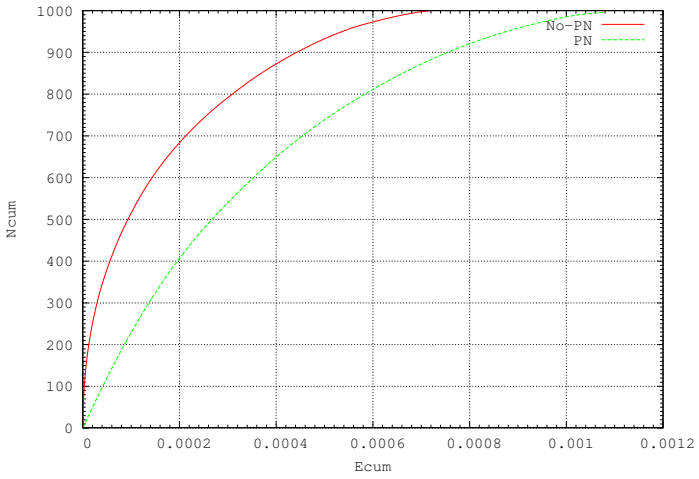

Figure 14: for t=2, $r_{per} = a_0$, cumulative energy

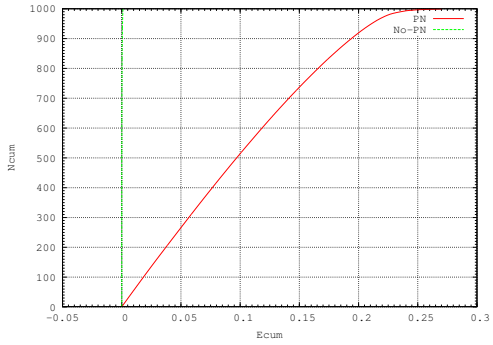

Figure 15: t=6, $r_{per} = 2a_0$

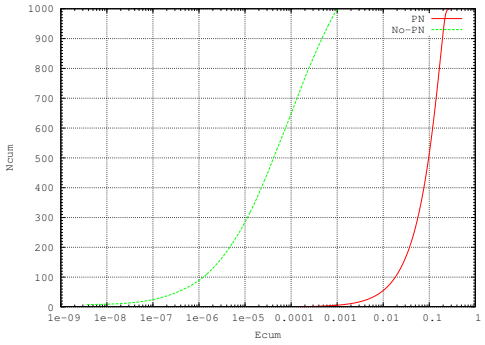

Figure 16: t=6, $r_{per} = 2a_0$(logscale)

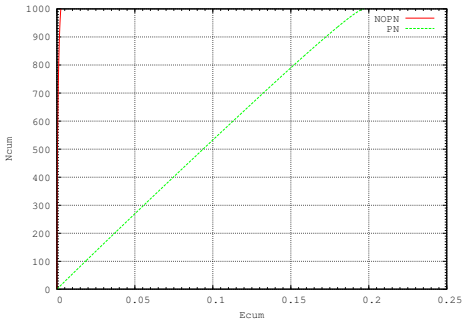

Figure 17: t=6, $r_{per} = a_0$

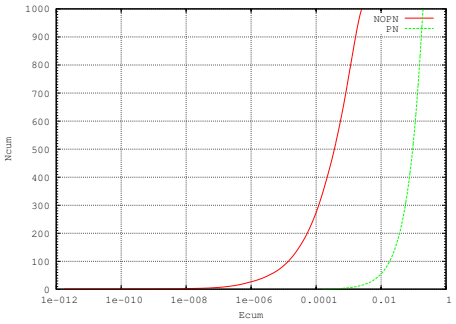

Figure 18: t=6, $r_{per} = a_0$(logscale)

As expected, from the above figures we can see that the energy difference between PN and NoPN is more prominent for t=6 case than the t=2 case. Also the cumulative PN energy change is more than the No-PN energy change.

NoPN comparison

We have compared here the No-PN cases for different times (t=2 and t=6) and also for different approach velocity of the intruder. The comparison plots are shown below.

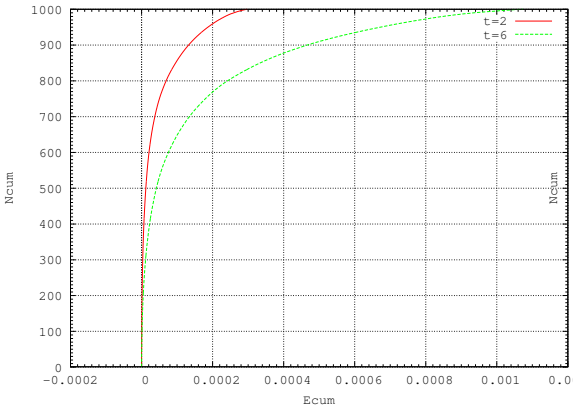

Figure 19: $r_{per} = 2a_0$

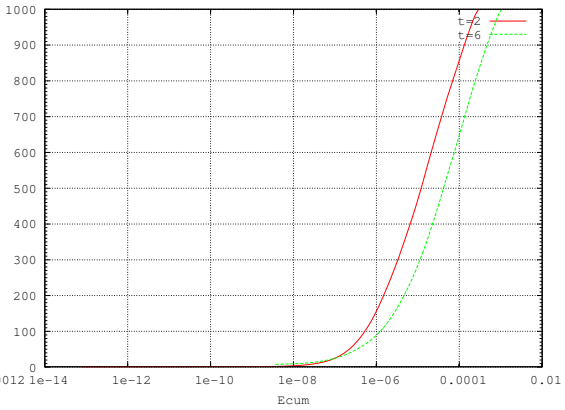

Figure 20: $r_{per} = 2a_0$(logscale)

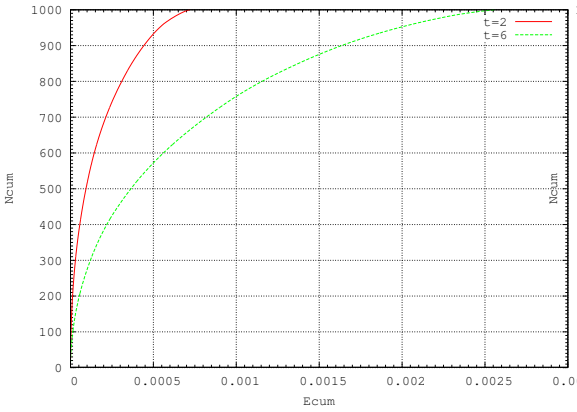

Figure 21: $r_{per} = a_0$

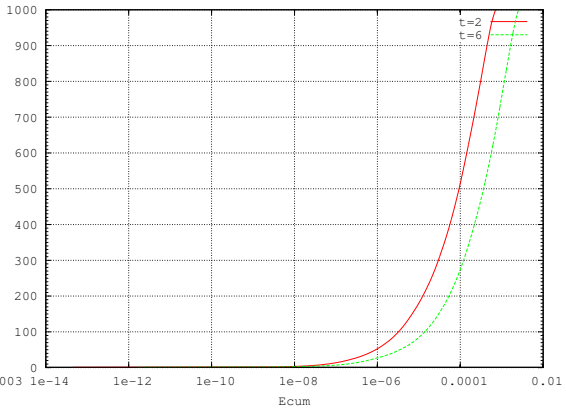

Figure 22: $r_{per} = a_0$(logscale)

So, even for the NoPN case the t=6 case represents more energy change. However if we look into the ratio of average energy change and initial energy ($\Delta E/E_0$), we get the following results.

$$\Delta E/E_0 = 2.411033655 \times 10^{-5} \text{ for t =2, } r_{per} = 2a_0$$
$$\Delta E/E_0 = 2.429431270 \times 10^{-5} \text{ for t =6, } r_{per} = 2a_0, \text{ and}$$

$$\Delta E/E_0 = 5.748491589 \times 10^{-5} \text{ for t =2, } r_{per} = a_0$$
$$\Delta E/E_0 = 5.781095833 \times 10^{-5} \text{ for t =6, } r_{per} = a_0$$

So, it's evident that the $\Delta E/E_0$ value is almost same for t=2 and t=6 cases for a given value of r_{per}, i.e., it does not depend on the time snap but as we can see

a significant difference between the simulations for different approach velocity of the intruder, i.e., for the $r_{per} = a_0$ case and $r_{per} = 2a_0$ case the $\Delta E/E_0$ value is quite different (almost double).

Now, we compare the NoPN cumulative plots for same time but different r_{per}.

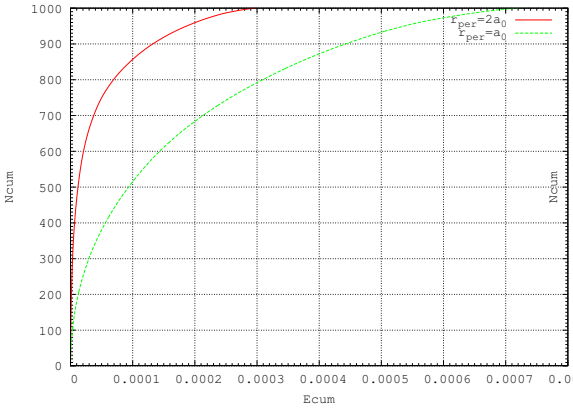

Figure 23: $t = 2$

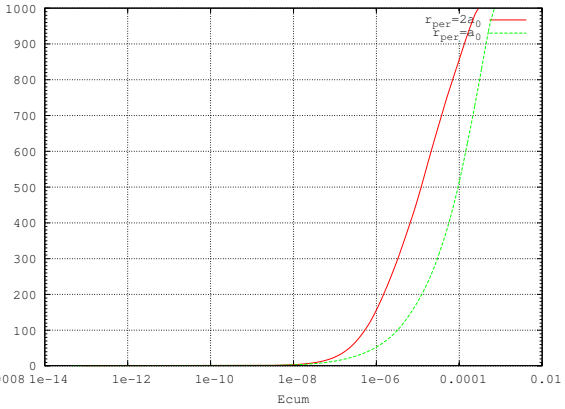

Figure 24: $t = 2$ (logscale)

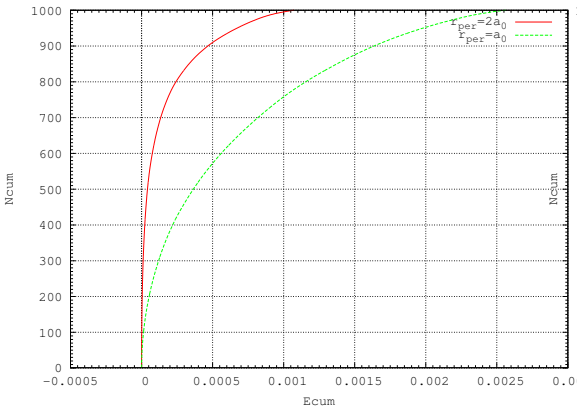

Figure 25: $t = 6$

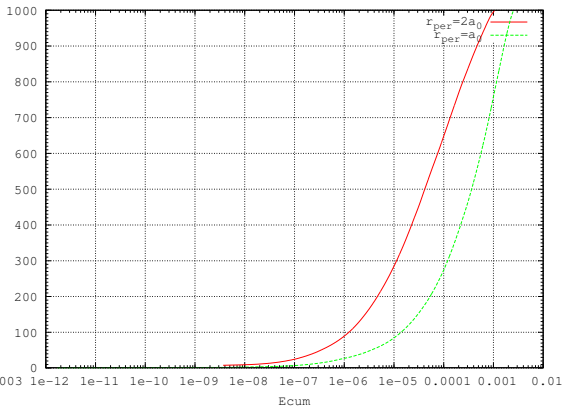

Figure 26: $t = 6$ (logscale)

Clearly the Newtonian energy change is larger for a_0 than for $2a_0$.

PN comparison

First the cumulative energy change for t=2 and t=6 is compared for a given r_{per}. As expected the t=6 instance indicates more energy change.

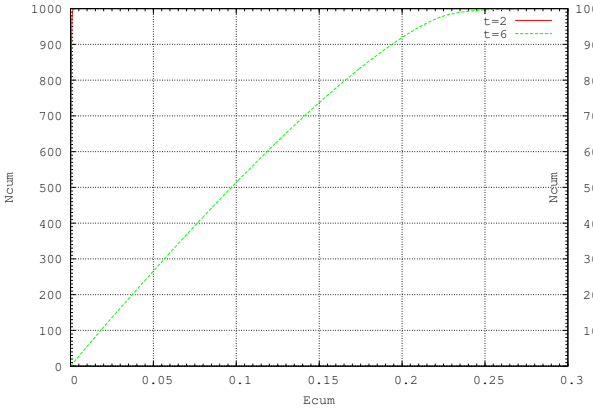

Figure 27: $r_{per} = 2a_0$

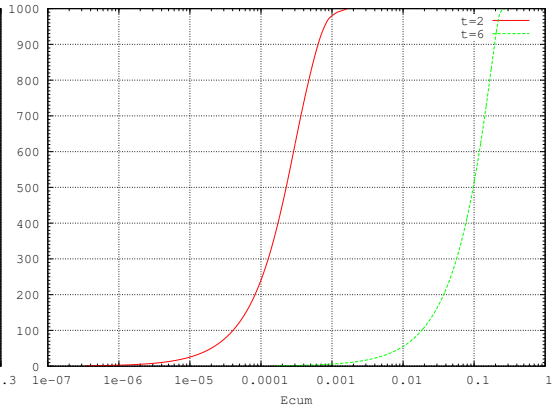

Figure 28: $r_{per} = 2a_0$ (logscale)

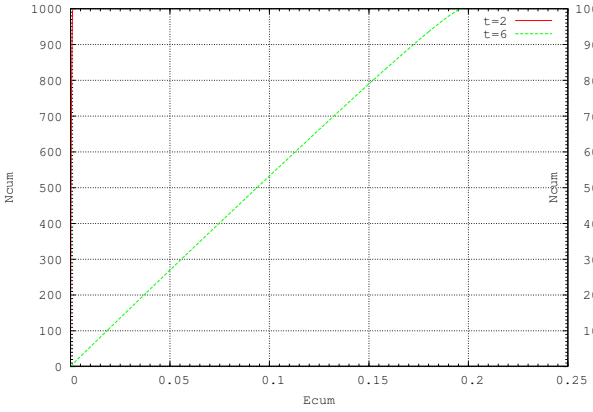

Figure 29: $r_{per} = a_0$

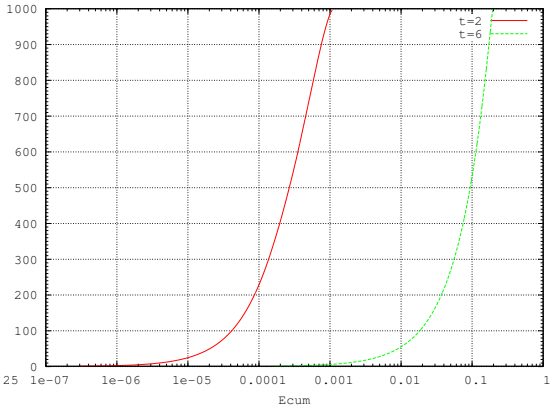

Figure 30: $r_{per} = a_0$ (logscale)

Now we compare the cumulative energy change for different pericenter distance but for a given instance (t=2 or t=6).

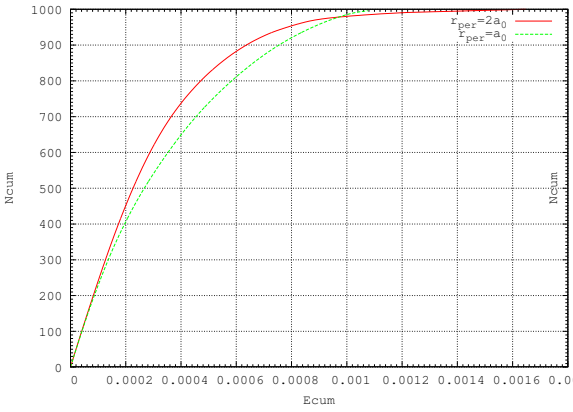

Figure 31: $t = 2$

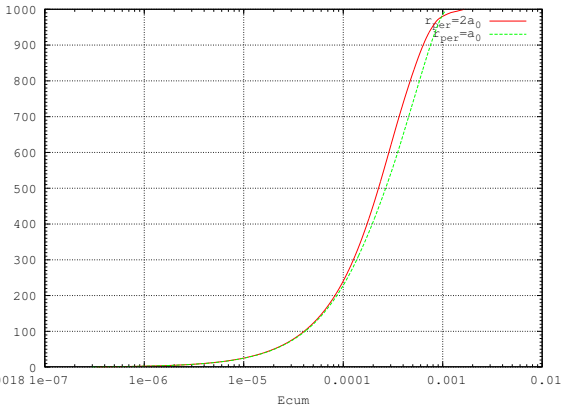

Figure 32: $t = 2$ (logscale)

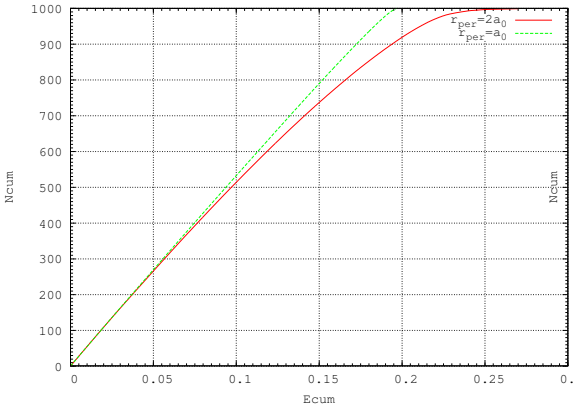

Figure 33: $t = 6$

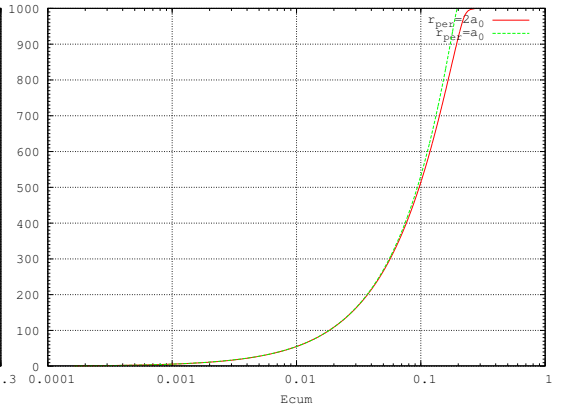

Figure 34: $t = 6$ (logscale)

Fig. 32 and Fig. 33 shows that the cumulative energy change is not much different for different pericenter distances. The dependence of binding energy on r_{per} is not very prominent. Another thing to observe is that, for the Newtonian case (NoPN), the cumulative energy change is dependent on r_{per} and for lower r_{per} we get more energy change. But in case of PN activated simulation, though the difference is very small, for higher r_{per} we get more energy change. This may be because of the fact that the time of interaction for a_0 case is less than the $2a_0$ case (for a_0, $t_{average} = 0.6165$, for $2a_0$, $t_{average} = 0.8114$).

3.7 Differential distribution

Now we want to see, how the amount of energy change is distributed. The plots in this section shows the frequency counts in the histograms of energy change.

NoPN comparison

We first compare the differential distribution for same pericenter distance but different binary time scale.

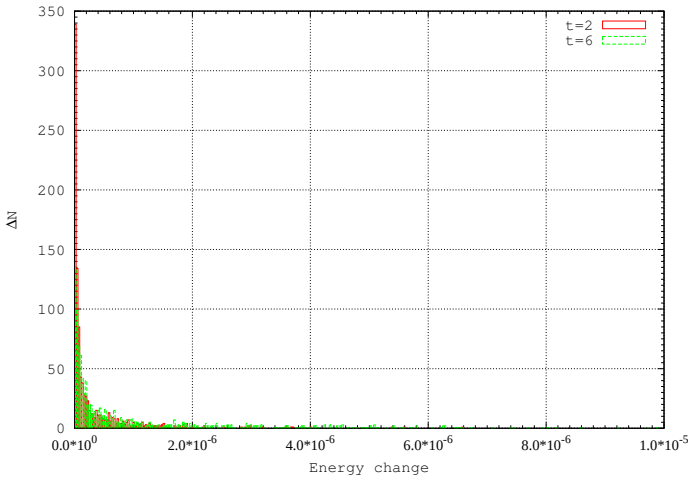

Figure 35: $r_{per} = 2a_0$ NoPN comparison

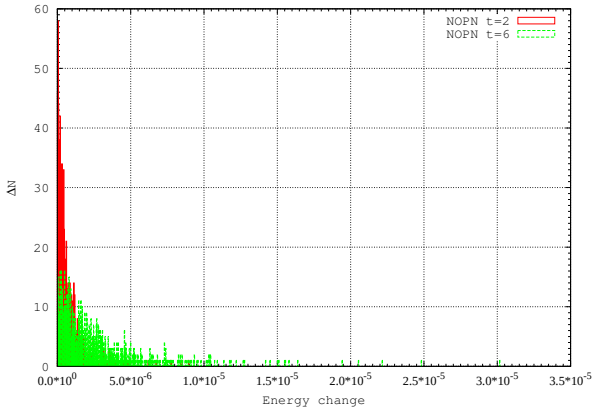

Figure 36: $r_{per} = a_0$ NoPN comparison

Now we compare NoPN diff. distributions for same time snap but for different pericenter distance.

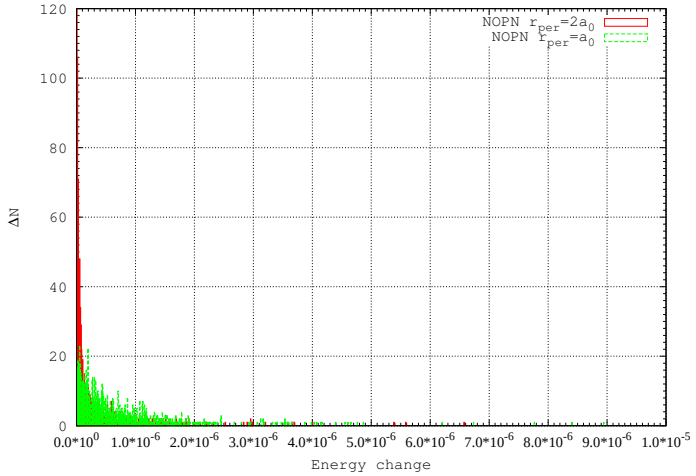

Figure 37: Comparison for t=2 but different r_{per}

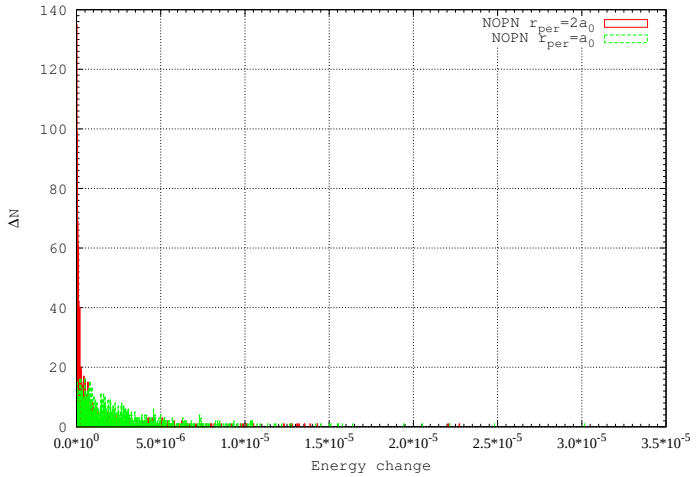

Figure 38: Comparison for t=6 but different r_{per}

PN comparison

First we compare for same pericenter distance but different time.

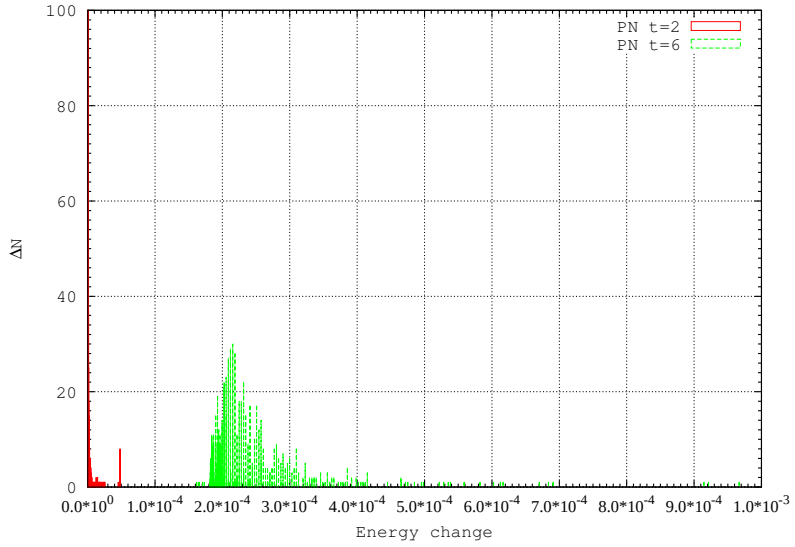

Figure 39: Comparison for $r_{per} = 2a_0$

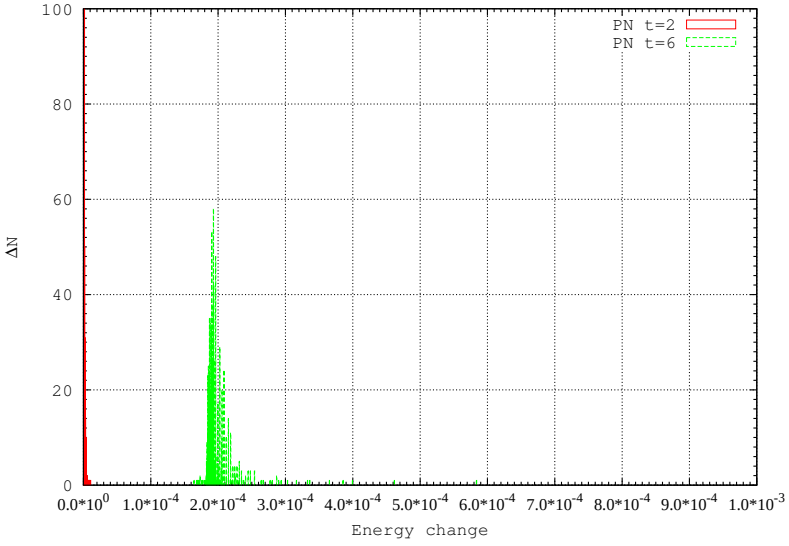

Figure 40: Comparison for $r_{per} = a_0$

Now we show the comparison of differential distribution for same time but for different pericenter distance.

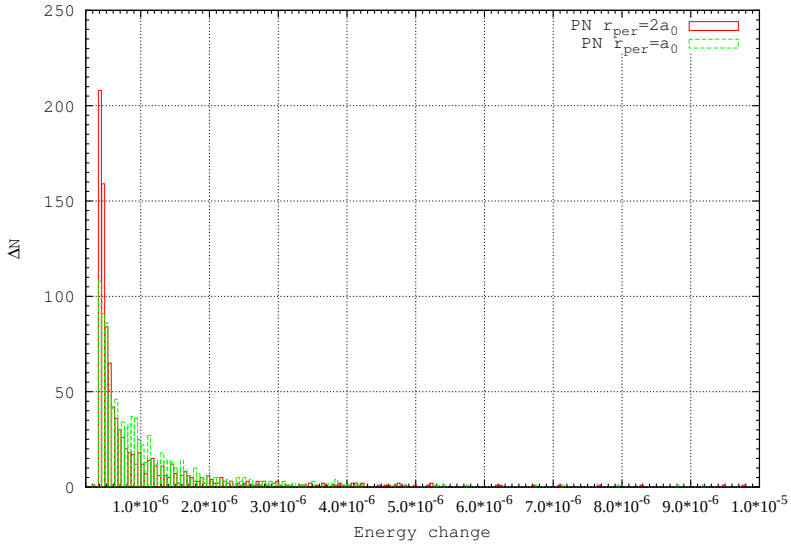

Figure 41: Comparison for t=2

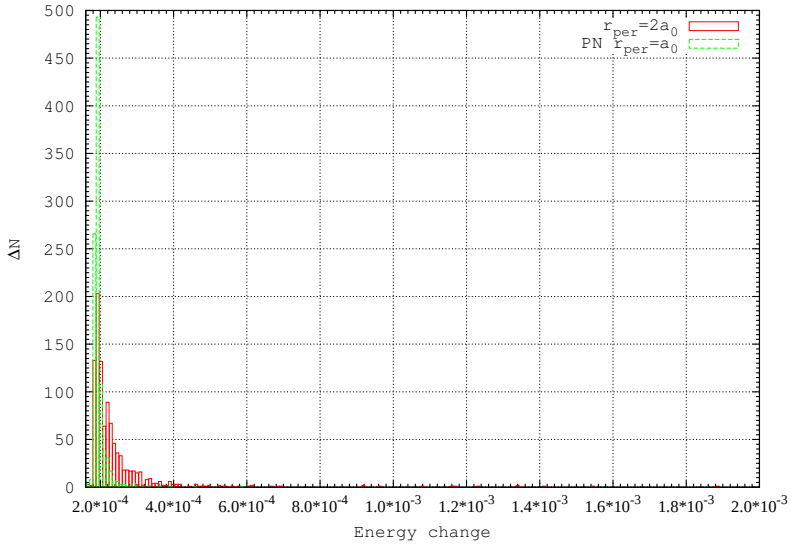

Figure 42: Comparison for t=6

PN NoPN comparison

We show in this section how the PN-NoPN differential distribution comparison looks.

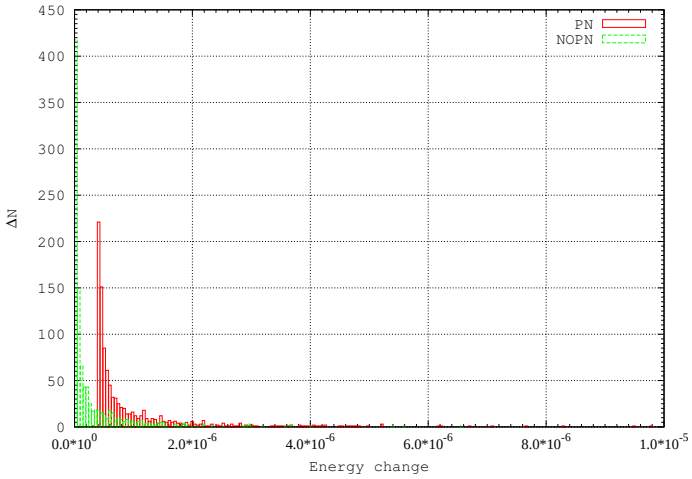

Figure 43: for t=2 and $r_{per} = 2a_0$

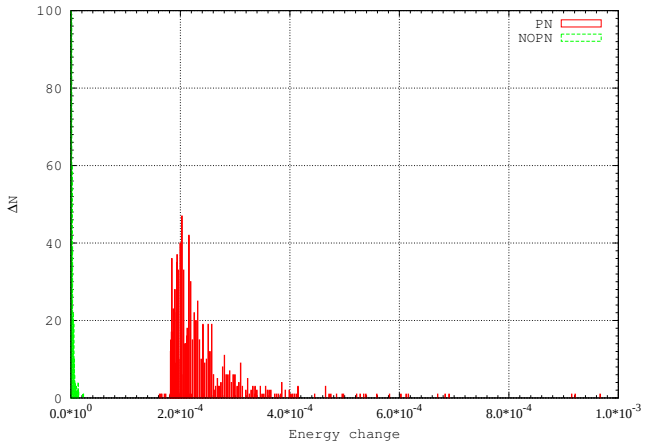

Figure 44: for t=6 and $r_{per} = 2a_0$

So, we see that for both PN and NoPN case the shape of the differential distribution is same but their origin is shifted giving the difference in energy change. The distribution looks like exponential decay, but a good fitting could not be obtained.

3.8 Newtonian Energy comparison

If we compare simply the Newtonian energy ($Gm_1m_2/2a$) for PN and NoPN cases, we get quite different results which shows that, it is incorrect to compare the Newtonian

energy of PN cases with the Newtonian energy of NoPN cases. In PN cases, the Newtonian binding energy can be both positive and negative depending on the intruder mass and time snap (for t=2 we get both positive and negative). Here we show cumulative Newtonian energy change comparison of PN and NoPN, for t=2 and t=6 case (Fig. 45 and Fig. 46).
So, we should consider the Newtonian+PN1+PN2 energy as the binding energy for the binary in the PN case.

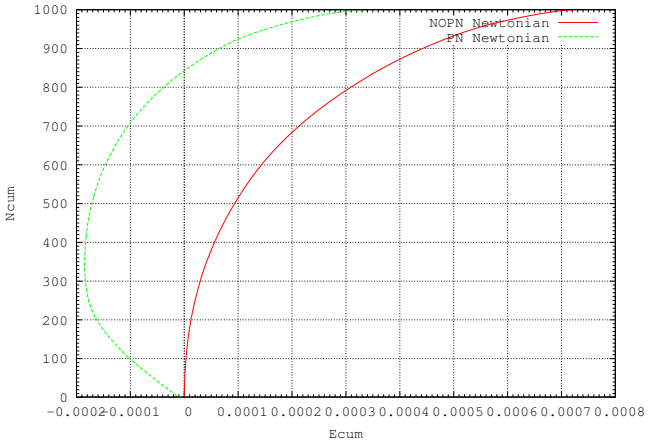

Figure 45: for t=2, $r_{per} = 2a_0$ Newtonian energy comparison

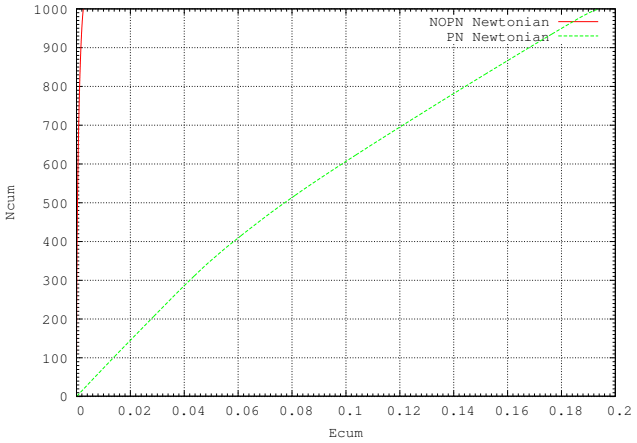

Figure 46: for t=2, $r_{per} = 2a_0$ Newtonian energy comparison

3.9 Effect of PN terms in corrected energy

Fig. 47 and Fig.48 shows the effect of the PN terms in cases of t=2 and t=6. To demonstrate the effect we have plotted the differential distribution of Newtonian energy and corrected energy for both the cases t=2 and t=6. The big tics on the X axis mark the expectation value of energy change.

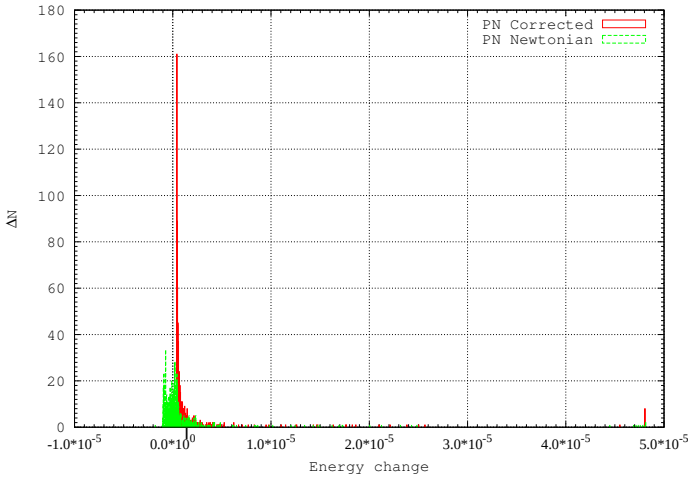

Figure 47: t=2 Comparison of Newtonian energy and Corrected energy

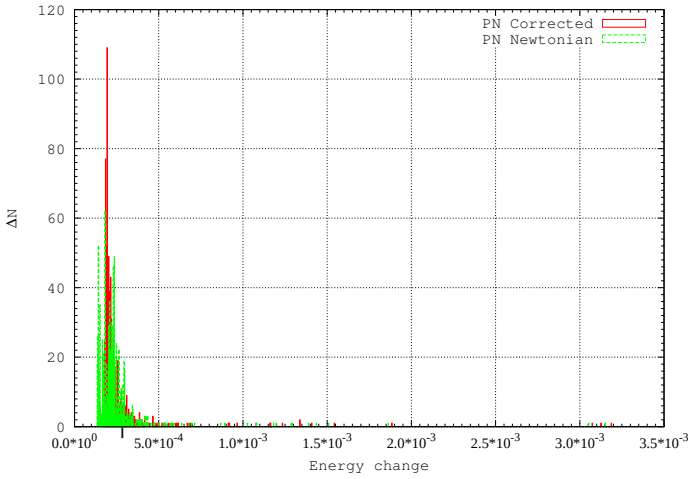

Figure 48: t=6 Comparison of Newtonian energy and Corrected energy

This shows that, though the effect of PN in case of t is very small, it is essential to

make the correction to get the right result. Otherwise we get negative energy changes in case of t=2 in disagreement of Heggie's Law.

3.10 Total star energy and Kinetic Energy of center of mass of BBH

A comparative plot of total star energy and K.E. of C.o.M of BBH variation with time for different cases is shown in Fig. 49 and Fig. 50.

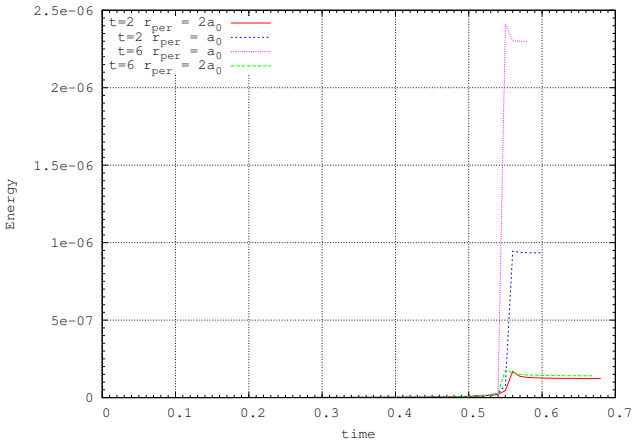

Figure 49: Total star energy comparison for different cases

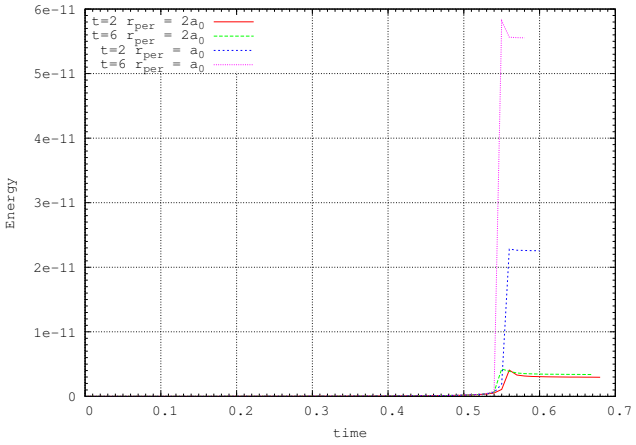

Figure 50: kin_{cm} comparison for different cases

We can see that the Kin_{cm} contributes a negligible amount of energy change to the system, so for all practical purposes we can neglect this energy.

3.11 With initial velocity of star tangential

We also have simulations with initial velocity of the stars only tangential (but same in magnitude), so that they follow a parabolic path on the way to encounter with the star. But we can see from the plots in this section that it does not affect the final energy change much.

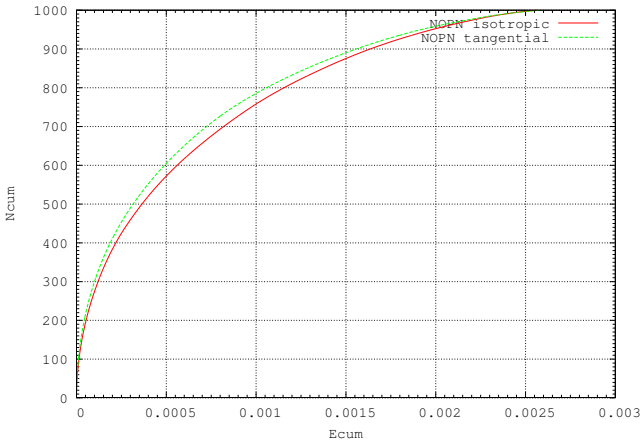

Figure 51: NoPN Cumulative energy change for t=6, $r_{per} = a_0$

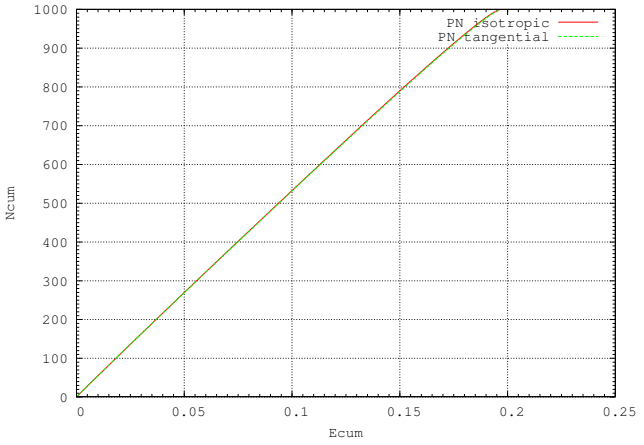

Figure 52: PN Cumulative energy change for t=6, $r_{per} = a_0$

So, we see that the initial direction of the velocity does not matter much.

3.12 Normalized Cumulative energy change

Till now we have shown the plots of cumulative energy change. Now, we plot the normalized cumulative energy change which is basically the plot of $(\Delta E)/E_0$, where E_0 is the initial binding energy. The plots are shown for both PN and NOPN cases.

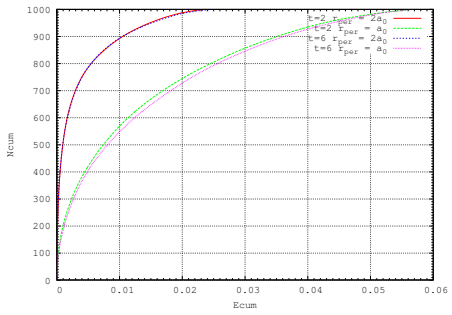

Figure 53: NoPN case

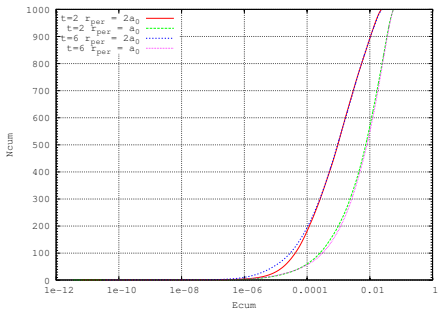

Figure 54: NoPN case (logscale)

Though they all should coincide, this may be because of the combined fact that about number of fly-by events are more and number of high energy interactions are less in the case of $2a_0$. So, we see a difference for the $2a_0$ and a_0 case. To somehow compensate this, we show the normalization plot where the normalization is done with the expectation value of $(\Delta E)/E_0$. The X axis now represents cumulative value of $\frac{(\Delta E/E_0)}{\langle \Delta E/E_0 \rangle}$.

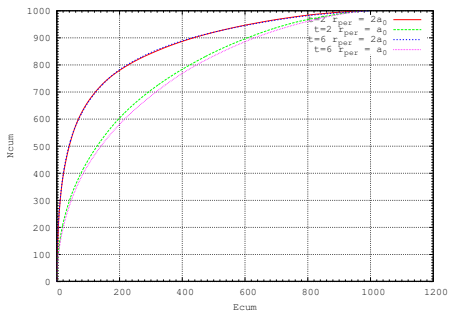

Figure 55: NoPN case normalized w.r.t. expectation value

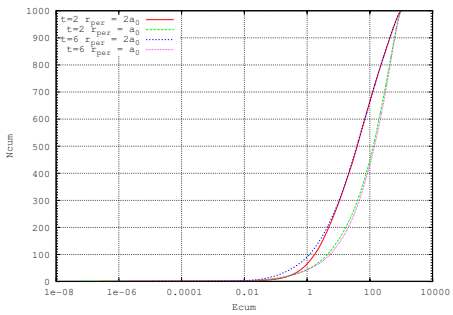

Figure 56: NoPN case normalized w.r.t. expectation value (logscale)

Similarly we show the plots for PN cases. (both normalized w.r.t. E_0 and w.r.t. $\langle \Delta E/E_0 \rangle$).

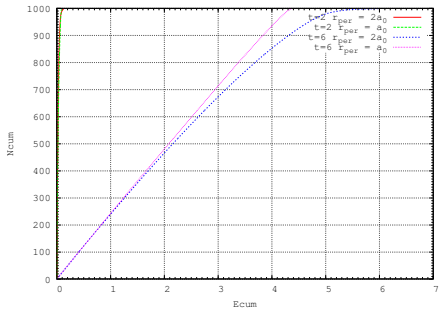

Figure 57: PN case

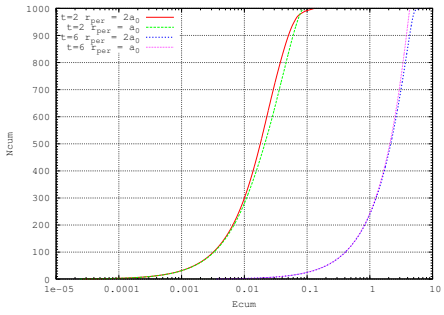

Figure 58: PN case (logscale)

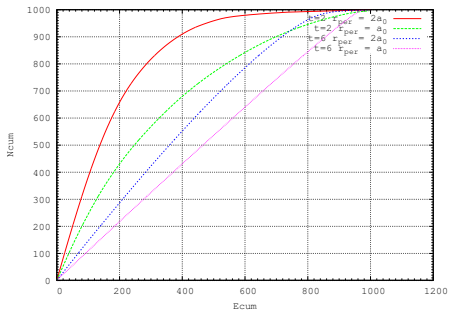

Figure 59: PN case normalized w.r.t. expectation value

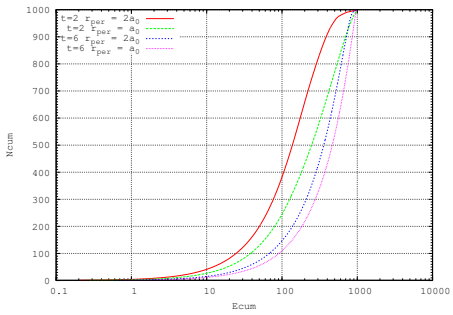

Figure 60: PN case normalized w.r.t. expectation value (logscale)

Here we observe a different pattern than the case of NoPN. The t=6 runs overlap and t=2 runs overlap. However for the normalized using expectation value plots, the difference is not very large.

3.13 Simulations for different masses

No-PN cases

Till now, for all the simulations, the intruder mass has been kept fixed. Now we vary the intruder mass. Three values of masses have been taken. These are $10^{-6}, 10^{-7}$, and 10^{-8} mass units. The simulations are done for both time t=2 and t=6 and for both PN and NoPN cases. Then the cumulative energy change and the normalized cumulative energy change (normalized w.r.t. mass, i.e. X axis represents $\Delta E/m_3$, where m_3 is mass of intruder) plots are shown in Fig. 61-64.

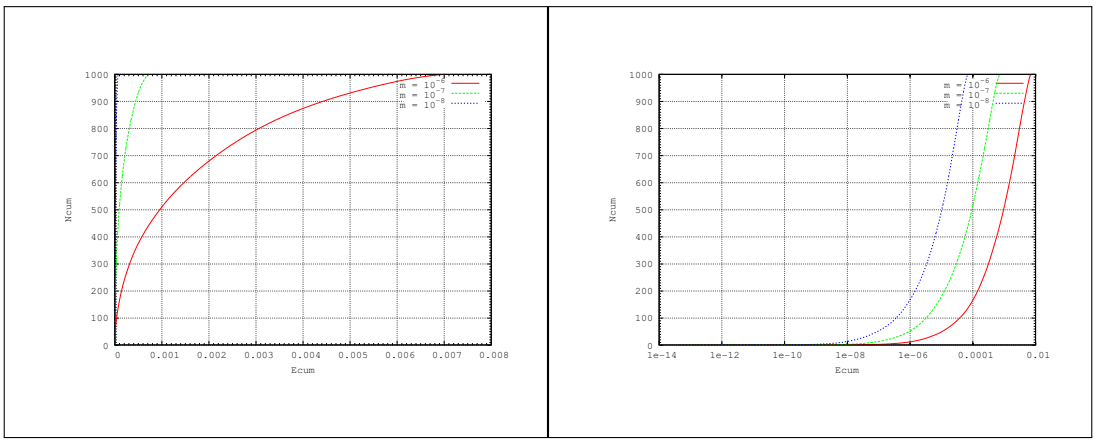

Figure 61: t=2 cumulative energy change for three different masses (linear scale and logscale)

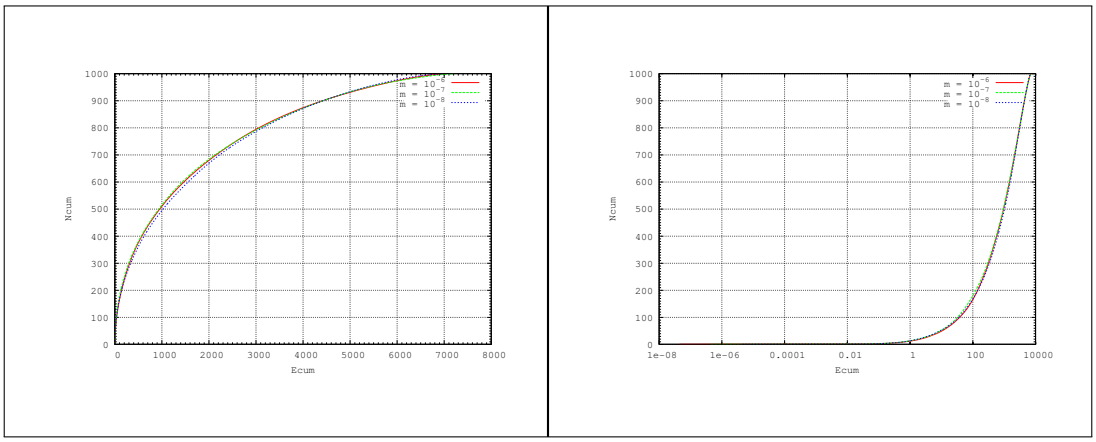

Figure 62: t=2 normalized cumulative energy change for three different masses (linear scale and logscale)

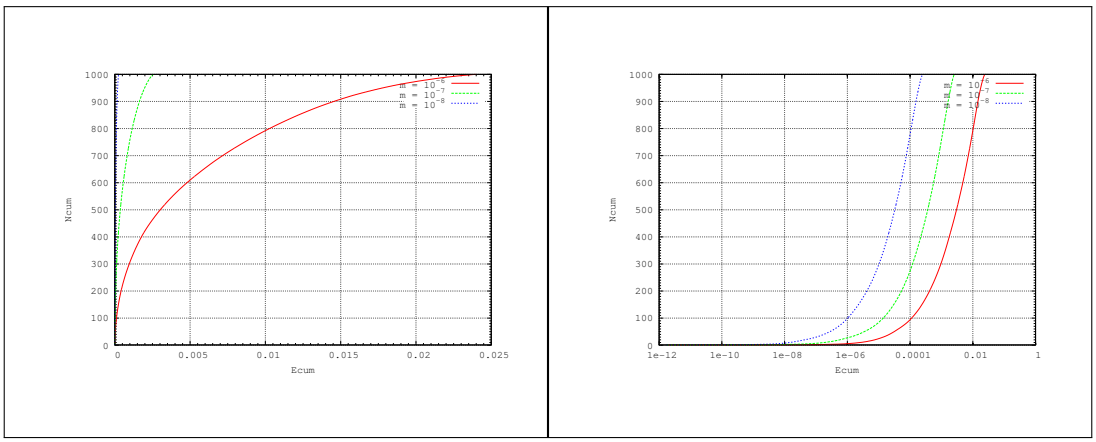

Figure 63: t=6 cumulative energy change for three different masses (linear scale and logscale)

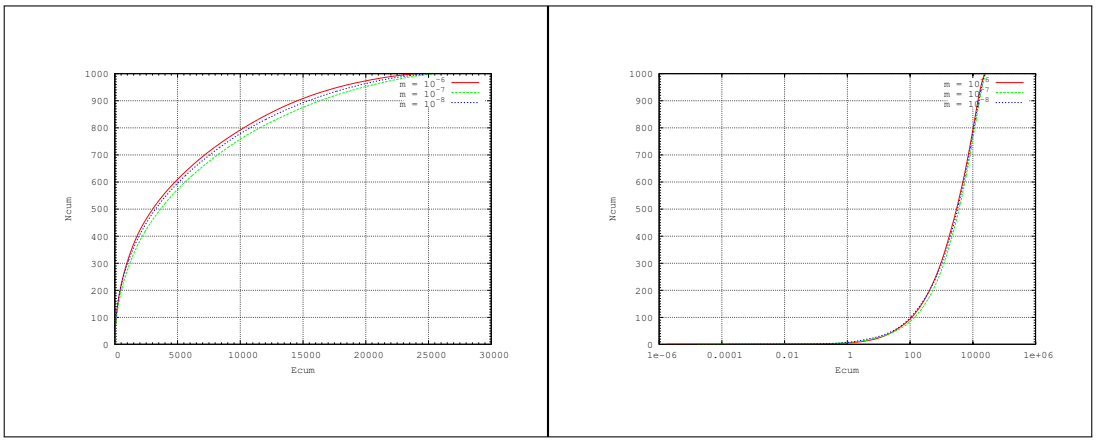

Figure 64: t=6 normalized cumulative energy change for three different masses (linear scale and logscale)

So, we see that the energy change for no PN case is directly proportional to the mass of the intruder. To show this dependence further we have plotted all the normalized curves in the same plot, (i.e. for both t=2 and t=6 and different masses) but now the normalization factor is (m_3/a_0), i.e. we have taken the initial energy into account as well in the normalization factor. Now all of them should co-incide as can be seen from fig.65.

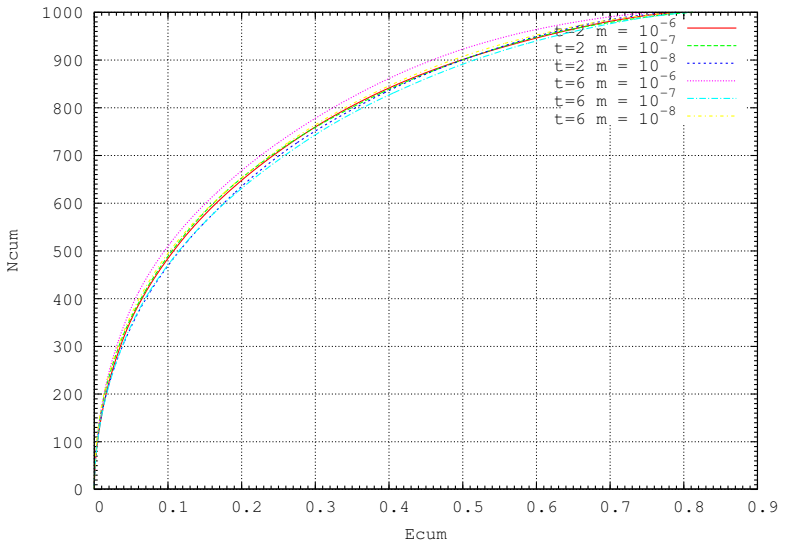

Figure 65: Normalized cumulative energy change w.r.t. both mass and initial energy

PN cases

We did the same simulation for the PN cases as well which resulted in Fig. 66-69.

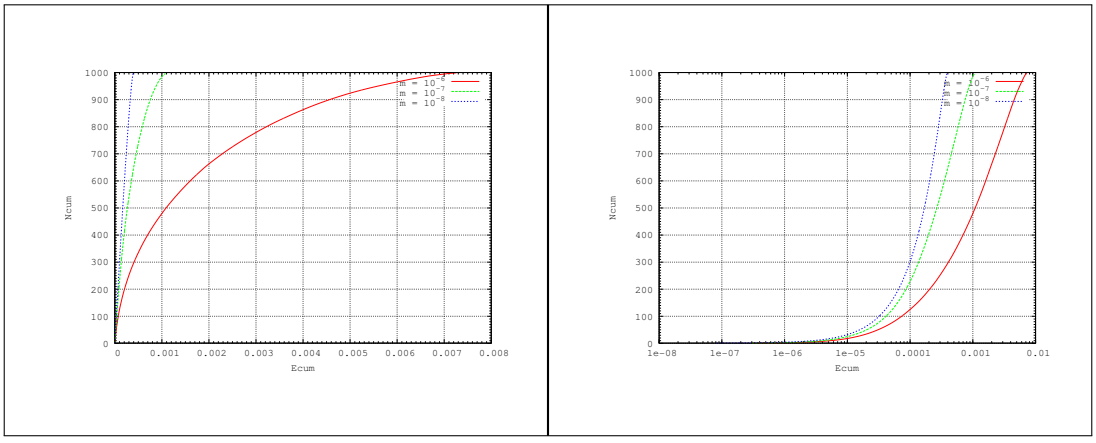

Figure 66: t=2 cumulative energy change for three different masses (linear scale and logscale)

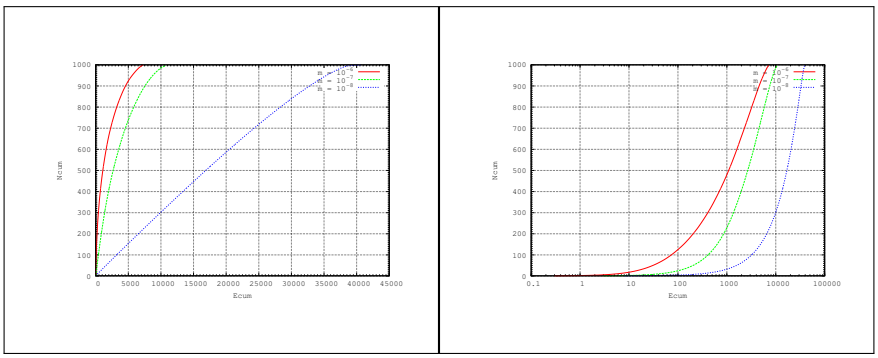

Figure 67: t=2 normalized cumulative energy change for three different masses (linear scale and logscale)

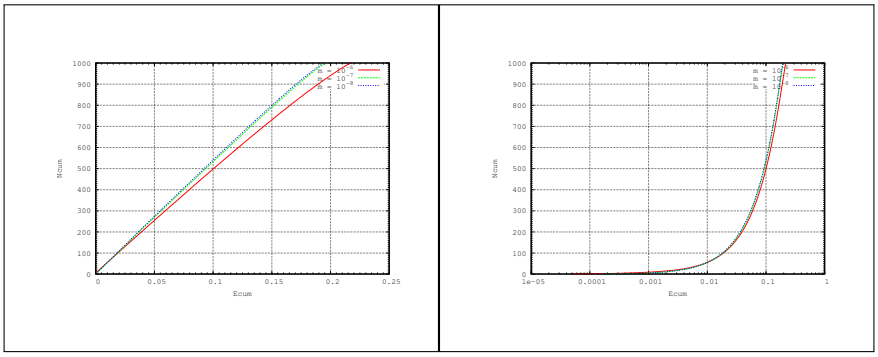

Figure 68: t=6 cumulative energy change for three different masses (linear scale and logscale)

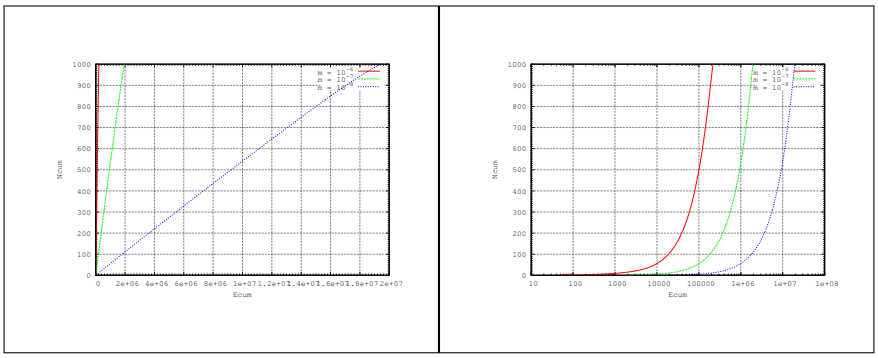

Figure 69: t=6 normalized cumulative energy change for three different masses (linear scale and logscale)

So, we see that the dependence of PN energy change on m_3 is not linear as was the case for No-PN. Also, after normalizing the order of energy change reverses which is an interesting thing to notice.

4 Simulation to see the frequency of fly-by events

For the No-PN cases, we have simulated the program for t=2, $m_3 = 10^{-7}$ and for different r_per. As the pericenter distance is increased, the probability of interaction decreases significantly. For $r_{per} = 4a_0$ only about 20% of the particles interact whereas for $r_{per} = 6a_0$ only 10% interact. So, to maintain efficiency of the program a_0 or $2a_0$ is the maximum safe pericenter distance. To show the comparison of cumulative energy change between a_0 run and $4a_0$ run we have shown Fig. 70. The plot shows that most of the events in $4a_0$ case is fly-by and hence very small energy change is noticed.

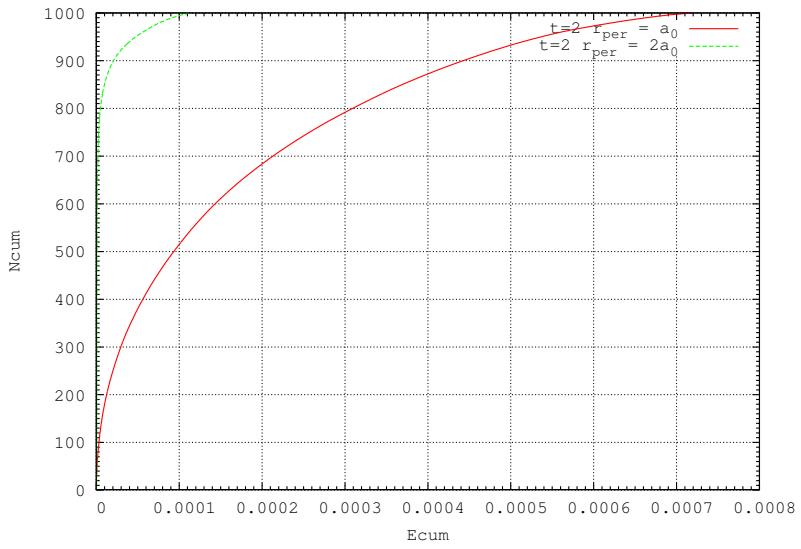

Figure 70: Normalized cumulative energy change w.r.t. both mass and initial energy

5 Results

Finally we summarize here the results of the simulations.

- The effect of PN is more evident for binaries in their later life stages.
- The effect of PN2.5 term is very small. It is only about 0.5% of the total energy.
- The cumulative energy change for NoPN case is dependent on the pericenter distance but for the PN case the dependence is very negligible.
- We see that the average $\Delta E/E_0$ value for NoPN is same for different time stages for a given pericenter distance but changes significantly for different pericenter distances.

- However for the PN case, the average $\Delta E/E_0$ value is dependent on both time and pericenter distance. The following values suggest this fact.

$$\Delta E/E_0 = 1.3670 \times 10^{-5} \text{ for t =2, } r_{per} = 2a_0$$
$$\Delta E/E_0 = 6.0016 \times 10^{-3} \text{ for t =6, } r_{per} = 2a_0, \text{ and}$$

$$\Delta E/E_0 = 8.53861 \times 10^{-5} \text{ for t =2, } r_{per} = a_0$$
$$\Delta E/E_0 = 4.47863 \times 10^{-3} \text{ for t =6, } r_{per} = a_0$$

- Number of high energy encounter is more in the case of $r_{per} = a_0$ than the case of $r_per = 2a_0$.
- In some cases (for t=2) we can see that the Newtonian binding energy change is negative rather than positive which indicates that the semi major axis of the binary is increased in the interaction rather than decreasing, thus contradicting the prevailing ideas. But if we consider the total PN energy, we see that the overall PN binding energy has increased (without considering the radiation energy loss). Thus we see that, the binary has become harder though there is a small increase in semi-major axis.
- Energy change in an interaction is linearly proportional to the intruder mass for no PN case but it is not for the case of PN interactions.
- The maximum pericenter distance for efficient program allowed, is $2a_0$. However a_0 is a better choice. Otherwise most of the encounters are fly-by.
- Though the PN terms are small compared to total energy for t=2 case, they are required for the correct energy value. Otherwise one gets negative binding energy change for interactions.

References

[1] Heggie, D.C., 1975, Binary evolution in stellar dynamics, *Monthly Notices of the Royal Astronomical Society*, **173**, 729.
[2] Mikkola, S., 2010, Algorithmic Regularization Chain (Presentation).
[3] Blanchet, L., Iyer, B.R., 2003, Third post-Newtonian dynamics of compact binaries: equations of motion in the centre-of-mass frame, *Class. Quantum Grav.*, **20**, 755.
[4] Peters, P.C., 1964, Gravitational radiation and the motion of two point masses, *Physical Review*, **136**, B1224.
[5] Blanchet, L., 2014, Gravitational Radiation from Post-Newtonian Sources and Inspiralling Compact Binaries, *Living Rev. Relativity*, 17, 2.